# Infrared and Ultraviolet–Visible Spectroscopy Study of the Degradation of Polyester and Polyester/Ethylene Methyl Acrylate Copolymer Blend Coatings on Steel

**Vanessa de Freitas Cunha Lins,[1] Flávia Medina Cury,[1] Roberto Moreira[2]**

[1]*Corrosion and Surface Engineering Laboratory, Chemical Engineering Department, Federal University of Minas Gerais, Rua Espirito Santo 35, 6th Floor, Belo Horizonte, Brazil 30160-030*
[2]*Department of Physics, Federal University of Minas Gerais, Presidente Antonio Carlos Avenue 6627, Belo Horizonte, Brazil 31270-010*

Received 22 June 2006; accepted 4 December 2007
DOI 10.1002/app.28231
Published online 2 May 2008 in Wiley InterScience (www.interscience.wiley.com).

**ABSTRACT:** Thermally sprayed polymer coatings have been used as protection against corrosion and wear. The aim of this study was to produce coated steel with a blend film with low-velocity combustion thermal spraying and a fusion technique and to evaluate its chemical degradation with infrared and ultraviolet–visible spectroscopy. The substrate used was carbon steel coated with recycled poly(ethylene terephthalate) (PET), an ethylene/methacrylic acid copolymer (EMAA), or PET–EMAA blends. The degradation of the material was evaluated with an ultraviolet condensation–weathering test and a salt-spray test. Measurements of hardness and adhesion were carried out. The tribological properties of the polymeric films were evaluated with a pin-on-disc test. © 2008 Wiley Periodicals, Inc. J Appl Polym Sci 109: 2103–2112, 2008

**Key words:** blends; coatings; FTIR; polyesters; recycling

## INTRODUCTION

Thermally sprayed polymer coatings have been used as protection against corrosion and wear.[1,2] Several polymers have been thermally sprayed, including polyethylene, the copolymer of ethylene and methacrylic acid, poly(methyl methacrylate), polyamide, and polyesters.[1,3,4]

In this study, recycled poly(ethylene terephthalate) (PET) and an ethylene/methacrylic acid copolymer (EMAA) were used as surface coatings on carbon steel with the purpose of obtaining a coating with corrosion resistance.

PET was chosen because its production is growing worldwide because of its utilization in soft drink bottles.[5] Several million tons of PET postconsumer plastic waste reaches the environment, and of this, only 7% is recycled to produce low-grade plastic product.[6]

EMAA was used because of its availability and known characteristics. EMAA has been used in coatings because of its versatility in different environments.[7] Its adhesive properties, already known, makes it useful for application on surfaces that require adhesion, such as in painting, skin protection, medical application,[8] and coated metal. The mechanism of interfacial interaction between EMAA and carbon steel consists of the interaction between the hydrogen of the hydroxyls of $Fe(OH)_2$ on the steel surface and the oxygen of the carboxyl.[3] The carboxyl disrupts the linearity of the polyethylene backbone, interferes as well with chain alignment, and reduces the total crystallinity, as in the case of other ethylene copolymers.[9] The acid functionality allows the polymers to form strong bonds to polar substrates.

The useful life of polymeric coatings depends on the rate and type of structural change that occurs during the time. If the polymer presents a visible change in its surface after the aging process, the material fails, even if there was no significant change in the material properties.[10] Degradation by environmental exposure is caused by radiation, temperature, humidity, and pollutants. Photon energy produced by ultraviolet light is a powerful source and is highly effective in breaking chemical bonds such as C—H and O—H.[11] Photodegradation may generate chemical groups such as carbonyl, carboxyl, and hydroperoxides.[12–14]

PET degradation has been extensively studied, and many mechanisms have been proposed to account for its various types of degradation,[15–21] but not many articles have been published about the

*Correspondence to:* V. de Freitas Cunha Lins (vanessa.lins@terra.com.br).

Contract grant sponsor: Conselho Nacional de Desenvolvimento Cientifico e Tecnológico.
Contract grant sponsor: Fundação de Amparo à Pesquisa do Estado de Minas Gerais.

photodegradation of PET.[22–24] The major reported products of the degradation of PET were carbon dioxide, acetaldeyde, vinyl benzoate, terephthalic acid, terephthaldeydic acid, and linear dimers.[25]

Blends of PET and EMAA showed compatibility[26] and toughness in several applications.[27]

In this article, steel coated with PET, EMAA, and PET/EMAA blends was analyzed with hardness and adhesion tests. The corrosion resistance of the coated steels was evaluated with salt-spray and weathering tests, and the degradation was evaluated with infrared and ultraviolet–visible spectroscopy. The tribological properties of the conjugates were evaluated with a pin-on-disk test. The results are discussed in terms of the changes in the coating structure that occurred during the experimental tests.

**TABLE I**
**Types of Polymeric Coatings**

| Sample | Symbol |
|---|---|
| 70% PET | 70PET |
| Aged 70% PET | 70PETA |
| Quenched 80% PET | 80PETQ |
| Quenched and aged 80% PET | 80PETQA |
| 80% PET | 80PET |
| Aged 80% PET | 80PETA |
| 90% PET | 90PET |
| Aged 90% PET | 90PETA |
| Thermally sprayed EMAA | EMTS |
| Thermally sprayed and aged EMAA | EMTSA |
| EMAA | EMAA |
| Re-fused EMAA | EMR |
| Re-fused and aged EMAA | EMRA |
| Quenched and aged PET | PETQA |
| Quenched PET | PETQ |
| PET | PET |
| Aged PET | PETA |

## EXPERIMENTAL

PET, EMAA, and PET–EMAA blend coatings were deposited onto ASTM A 36 steel with a thermal spray and fusion technique. The chemical composition of the steel used in this research was 0.26% C, 0.4% Si, 0.2% Cu, and 0.8% Mn (w/w).

Table I shows the several types of polymeric coatings studied in this investigation. The mixtures of PET and EMAA contained about 70–90% (w/w) PET.

The blasting of steel samples was carried out with an air pressure of $3.10^5$ N/m$^2$, and the abrasive material was aluminum oxide. The roughness of the samples was measured with a Taylor–Hobson subtronic 3+ model HB-103 surface profilometer (Paoli, PA). The samples were submitted to pickling with a 50% v/v HCl solution with hexamethylene tetramine as an inhibitor.

The steel samples were placed in a furnace at a temperature higher than the melting temperature of the polymer for 10 min. The furnace was opened, and the polymer (PET or EMAA) powder was scattered on the steel surface. The samples then remained in the furnace at the melting temperature of the polymer for 10 min. In the case where the powder was a mixture of PET and EMAA, the smaller polymer melting temperature was used. After fusion, the samples were air-cooled. The steels coated with PET and 80% PET/20% EMAA were also quenched in an ice–water mixture at 0°C.

The EMAA coatings were thermally sprayed on carbon steel sheets.

The substrates were gritted blasted with aluminum oxide immediately before thermal spraying. The coatings were applied with a Metco PerkinElmer flame-spray system (Waltham, MA) with a diamond-jet-type, low-velocity oxyfuel torch. The powder feed was carried out with a type DJP fluidized hopper from Metco PerkinElmer. Nitrogen at $689.3 \times 10^3$ N/m$^2$ was used as the carrier gas, and the PET powder was fed at a rate of 0.16 g/s. The fuel was propane gas injected at variable flow rates. The propane pressure was $275.7 \times 10^3$ N/m$^2$, and the flow rates were 7.4 and $14.2 \times 10^{-6}$ m$^3$/s. The oxygen pressure was $344.7 \times 10^3$ N/m$^2$, and the compressed air pressure was $206.8 \times 10^3$ N/m$^2$. The substrate temperature was 82°C.

Coating hardness was measured with a Shore D machine (Instron, Elancourt, Cedex, France), according to the NBR 7456 standard. Five measurements of hardness were taken for each sample, and the average value was recorded.

The adhesion test was carried out according to Associação Brasileira de Normas Técnicas standards with an Elcometer (model 106, scale number 3, series ND 3013) (Pompano Beach, FL). A steel pin was fixed on the surface of the sample with a commercial glue. The drying time was 24 h. After drying, the machine pulled up the pin, and the rupture force was recorded.

The salt-spray test was performed according to ASTM D 117 for 166 h. The samples were scratched with a tungsten carbide instrument to expose the substrate. Measurements of the corrosion propagation were taken, which was observed in relation to the scratch.

The weathering test was carried out with Weather-O-Meter equipment (Atlas Handling Systems, Kansas City, MO), according to ASTM G 53 over 807 h. The samples were exposed to ultraviolet light at 70°C for 8 h, and then, they were submitted to condensation conditions at 50°C for 4 h. Steel sheets with dimensions of $10 \times 8$ cm$^2$ and a thickness of 3 mm were coated and used in the weathering test.

The equipment used for Fourier transform infrared (FTIR) spectroscopy was a Thermo Nicolet

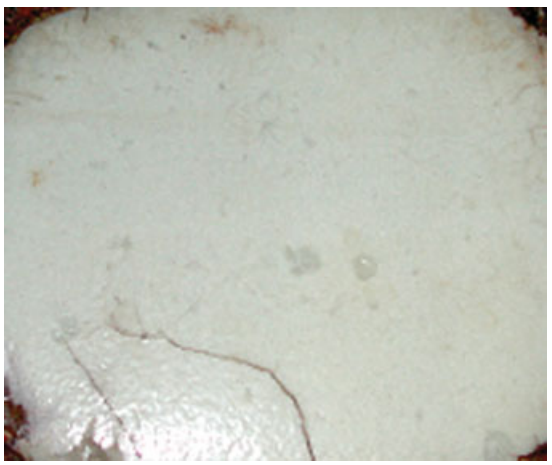

**Figure 1** Air-cooled, PET-coated steel surface after exposure in the weathering chamber. [Color figure can be viewed in the online issue, which is available at www.interscience.wiley.com.]

NEXUS 470FTIR instrument (Waltham, MA). Two measurements were done. First, a piece of coating with an appropriate thickness was analyzed. In the second test, the micro-attenuated total reflection technique was used, with a ZnSe crystal coupled to the microscope. The second test, with the ZnSe crystal, was realized only for the following samples: thermally sprayed EMAA before the aging test, re-fused EMAA before and after the aging test, air-cooled re-fused PET, and quenched re-fused PET after the aging test. The other samples showed characteristics of porosity and roughness that generated poor contact between the ZnSe crystal and the polymer surface.

The equipment used for ultraviolet–visible spectroscopy was a Shimadzu UV 2401PC instrument. The reflectance method was used, with an angle of 5°. There was a change of detector at the wave number 740 nm and an alteration from the tungsten lamp to the deuterium lamp at the wave number 360 nm. The samples used in the FTIR and ultraviolet–visible spectroscopy had dimensions of 2 cm in length and 2 cm in width. The samples analyzed were cleaned with isopropyl alcohol.

The pin-on-disk test was performed according to ASTM G 99. Some pins made of chrome steel were the test specimens, and the sample was the counterweight. The conjugated surface was parallel to the disk plane. Each test made 8024 revolutions, or 350 m, under 10 N of applied force.

## RESULTS AND DISCUSSION

The use of a fusion technique is limited by the kiln size, which limits the sample size. The average thickness of the polymeric coatings was 1 mm. The thermal spraying technique does not have important or significant limitations, it can be carried out anywhere, and any sample size can be used as long as the equipment can be easily transported.

The PET coatings were only produced with the fusion technique. When the coated plate was not quenched, the coating surface usually presented cracks (Fig. 1). The quenched PET coating was amorphous and transparent.

### Hardness and adhesion measurements

Amorphous EMAA coatings showed the smallest hardness value of all of the samples (Fig. 2). The hardnesses of quenched PET and 80% PET/20% EMAA coating samples were lower than the hardness of the same composition air-cooled coating samples (Fig. 2).

The adhesion of the coatings to the substrate was higher than 8 MPa, which was evaluated with the Elcometer test.

### Salt-spray test

During the salt-spray test, some visual observations were performed to identify corrosion specks on the surface of coated steels. The samples showed no propagation of corrosion from the scratch. PET coating samples and 80% PET/20% EMAA and 90% PET/10% EMAA coating samples showed specks on their surface after 117 h of testing. PET blends that were quenched after re-fusion showed no surface alteration after exposure for 166 h in the salt-spray chamber. Quenched PET blends with 80% PET showed the highest corrosion resistance after 117 h of exposure in the salt-spray chamber. Air-cooled PET coatings showed cracks and rust specks after 9 h of testing.

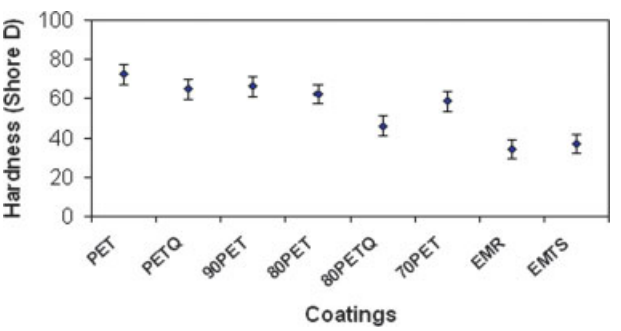


**Figure 2** Hardness of the PET and PET–EMAA blend coatings (see Table I for definitions of the symbols). [Color figure can be viewed in the online issue, which is available at www.interscience.wiley.com.]

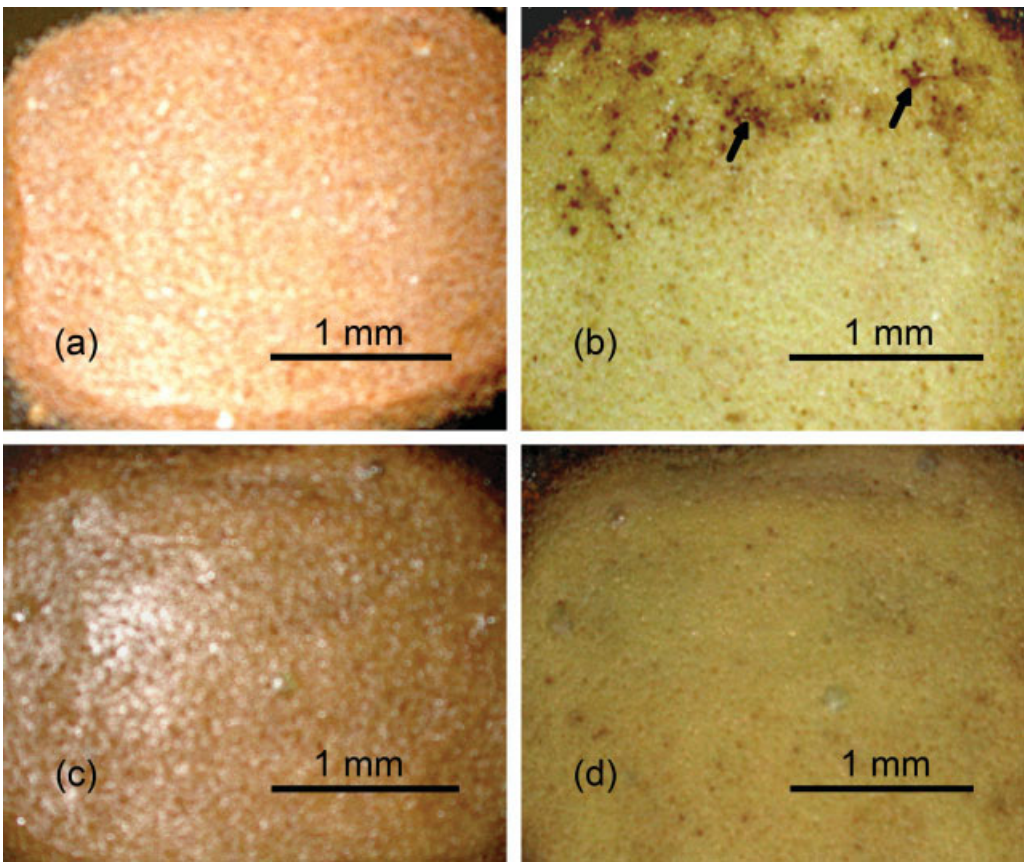


**Figure 3** Air-cooled, 80% PET/20% EMAA coated steel surface (a) before and (b) after the aging process and quenched, 80% PET/20% EMAA coated steel surface (c) before and (d) after the aging process. [Color figure can be viewed in the online issue, which is available at www.interscience.wiley.com.]

### Weathering test

The re-fused and thermally sprayed EMAA coatings did not show visible alterations after the aging process but presented a loss of brightness after exposure in the weathering chamber.

The re-fused 70% PET/30% EMAA blend coatings presented a color change after exposure in the weathering chamber. The aged surface showed a clear yellow color with brown spots. The air-cooled [Fig. 3(b)] and quenched [Fig. 3(d)] re-fused 80% PET/20% EMAA coated steels showed a clear yellow color with brown spots and black points on the polymeric surface after the aging process. The air-cooled 80% PET/20% EMAA coatings [Fig. 3(b)] also showed more brown and black spots on the surface than the quenched 80% PET coatings [Fig. 3(d)]. The small black spots were probably associated with the pores, which allowed the corrosion products of steel to reach the surface. The substrate of carbon steel exposed in the weathering chamber to the wet atmosphere through pinholes could have generated the red rust, or iron oxides/hydroxides, visible on the surface.[28] SEM analysis identified the presence of iron in brown-spot regions of the surface of air-cooled 80% PET coated steel after the weathering test. The brown spots were not restricted to the pore areas on the polymeric surface and should have been due to the chemical alterations of the polymers. Studies carried out by Edge et al.[20,21] suggested that color formation starts with the hydroxylation of the terephthalic ring producing hydroxylated species, which on further oxidation, leads to quinonoid-type structures. The 90% PET/10% EMAA coated steels also showed a color change, with the appearance of a light yellow color on the surface with a few spots on the polymeric surface.

The air-cooled PET coated steels showed cracks after the aging process (Fig. 1), with brown color in the crack area and in a few points associated with the pores on the surface.

### FTIR analysis

In the spectra of the poly(methacrylic acid), a wide band between 3200 and 2600 $cm^{-1}$ due to the deformation of O—H of carboxyl was identified. The peak between 1700 and 1750 $cm^{-1}$ occurred because of a C=O deformation of the carboxyl. Peaks at 1480

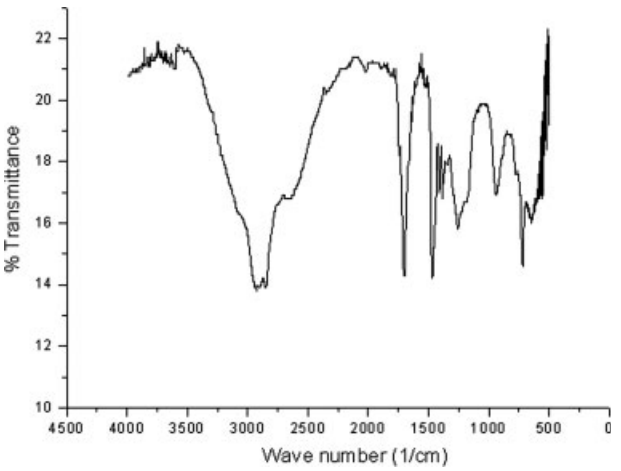


**Figure 4** FTIR spectrum of EMAA powder.

and 1460 $cm^{-1}$ were related to the $CH_2$ and $CH_3$ groups of the polymer, and the peak at 1260 $cm^{-1}$ concerned the absorption of the C—O group. Peaks at 940 and 960 $cm^{-1}$ occurred in a weak form because of the angular deformation outside the plan of the O—H bond in the hydrogen bond and occurred as a double peak because of the presence of the C=C group, a deformation of the polymeric chain that appeared as a defect of the polymer.[29] In the spectra of poly(methacrylic acid), a 2600-$cm^{-1}$ band related to the C—$O_2$ bond and a peak at 3000 $cm^{-1}$ related to the $CH_2$ and $CH_3$ groups were observed.[29]

In the spectra of polyethylene, the peak at 2800–3000 $cm^{-1}$ was due to the deformation of C—H, and the peak at 1480–1460 $cm^{-1}$ was related to the $CH_2$ group. The double peak at 720 and 730 $cm^{-1}$ occurred because of the association in long sequences of the $CH_2$ group.[29]

The spectra of the EMAA powder is shown in Figure 4. Bands at 3000 and 2800 $cm^{-1}$ overcame the bands at 3200 and 2600 $cm^{-1}$ because the axial deformation bands of C—H of alkyl were weaker and were overcome by the large band of O—H. The fine structure observed on the side of higher wave numbers of the O—H band was generally due to the harmonic bands and combination bands that occurred at the highest wave numbers.[29] As shown in Figure 4, a 2600-$cm^{-1}$ band corresponding to the C—$O_2$ bond and a 3000-$cm^{-1}$ peak associated with the $CH_2$ and $CH_3$ groups were identified. Peaks at 1700, 1750, 1260, and 940 and 960 $cm^{-1}$ were also present, but the peak around 960 $cm^{-1}$ appeared as a single one. Probably, the EMAA polymerization under high pressure and with free radicals generated defects in the polymer chains. Peaks at 1480 and 1460 $cm^{-1}$ appeared to overcome to each other. Observed in the EMAA powder were peaks that were characteristic of polyethylene and poly(metacrylic acid).

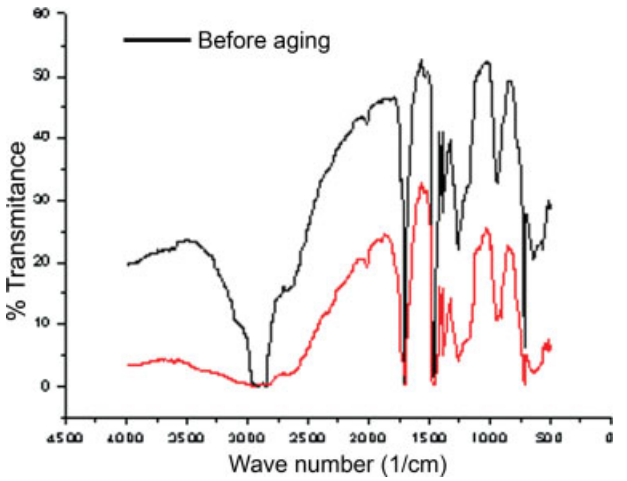


**Figure 5** FTIR spectra of the re-fused EMAA coated steel before and after the aging process. [Color figure can be viewed in the online issue, which is available at www.interscience.wiley.com.]

The spectra of the re-fused EMAA was similar to the spectra of the EMAA powder (Fig. 5). Peaks at 940 and 960 $cm^{-1}$ appeared in the spectra of the re-fused EMAA before the aging as a single peak and after the aging process as a double peak. The intensity of the broad band around 3500 $cm^{-1}$ decreased after the re-fusion process.

The spectrum of the thermally sprayed EMAA coating on steel was similar to the spectrum of the EMAA powder (Fig. 6). After the aging process, the duplications of the peaks at 1260 and 940 and 960 $cm^{-1}$ were observed (Fig. 6). The peak at 1260 $cm^{-1}$ was associated with the C—O bond, which may have been formed because of the cross-linking process. Peaks at 960 and 940 $cm^{-1}$ were asso-

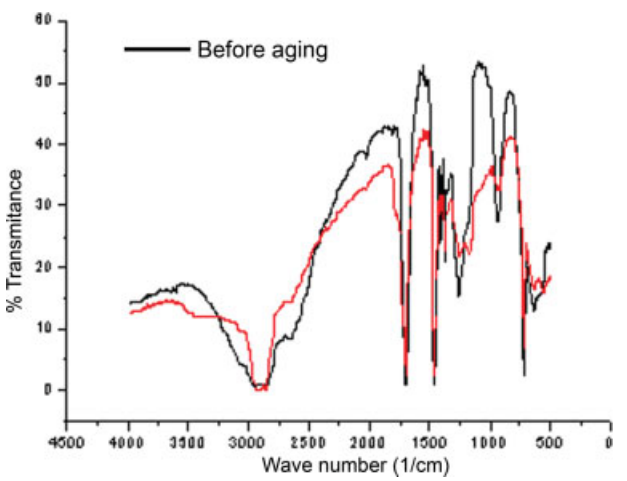


**Figure 6** FTIR spectra of the thermally sprayed EMAA coated steel before and after the aging process. [Color figure can be viewed in the online issue, which is available at www.interscience.wiley.com.]

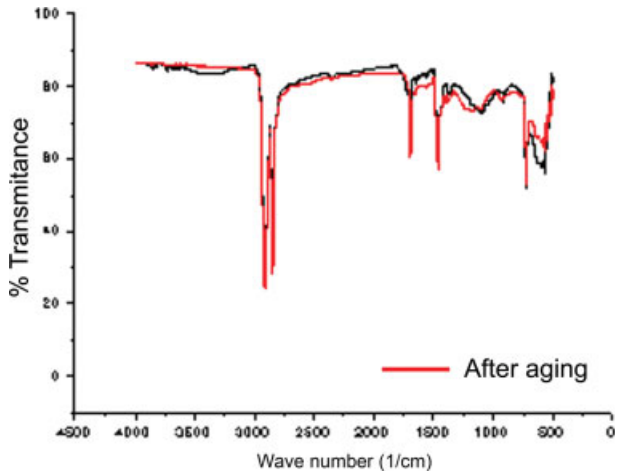


**Figure 7** Spectra obtained with the ZnSe crystal test of the re-fused EMAA before and after the aging process. [Color figure can be viewed in the online issue, which is available at www.interscience.wiley.com.]

ciated with the O—H and may have appeared because of the hydration of the carboxyl. In fact, the intensity of the peaks at 1700–1750 $cm^{-1}$ associated with the C=O functional group decreased after the aging process in the weathering chamber (Fig. 6).

In a previous work,[30] a decrease of the strain at break was observed after the aging process. EMAA coatings produced by a re-fusion technique showed the highest elongation of 158% for the coating before aging and a value of 65% for the aged polymeric coating. Oreski and Wallner[31] cited the strain at break as the most sensitive parameter for evaluating the degradation effects of the aging test. If a crosslinking process occurred with the polymeric molecular chains or a hydrogen bond network occurred, the elongation would decrease after exposure in the weathering chamber, as observed.[30]

In the test with the ZnSe crystal of the re-fused EMAA before and after the aging process (Fig. 7), peaks at 2800–3000, 1700–1750, 1480, 1260, 940–960, and 720–730 $cm^{-1}$ were identified. Peaks at 1260 and 940–960 $cm^{-1}$ of the re-fused EMAA showed changes before and after aging (Fig. 7). Before the aging process, these peaks were broad, and after exposure in the weathering chamber, these peaks became tight. The peak associated with the C=O of the carboxyl acid became weak in the spectrum of re-fused EMAA after aging. During aging, the UV radiation could have broken down the chemical bond C=O in the polymer chain and generated crosslinking or hydration with the carbon linking to hydroxyls.

The peaks at 3550 $cm^{-1}$ that was associated with the absorbed moisture and the peak at 3650 $cm^{-1}$ that appeared in the spectra of PET powder did not appear in the PET coating spectra. In the PET powder spectrum (Fig. 8), the band at 3440 $cm^{-1}$ represented the O—H groups of the carboxyl and hydroxyl ester. The O—H linked to the carbonyl and the O—H linked to the aliphatic chain absorbed at different wave numbers and produced a double peak at 3440 $cm^{-1}$. However, in the PET spectrum, a single peak appeared, and it was related to the O—H of hydroxyl ester that appeared in higher quantities than the O—H of the carbonyl.[32,33] In the PET spectrum, bands at 2960–2880 $cm^{-1}$ were related to the aliphatic C—H stretching, and peaks at 3060 $cm^{-1}$ were assigned to the aromatic C—H stretching. A peak related to the deformation of C=O of esters (1730 $cm^{-1}$) and a peak due to the stretching of C(=O)O of esters (1270 $cm^{-1}$) were identified (Fig. 8). A peak associated with the deformation of O—$CH_2$ of the ethylene glycol segment in PET and a peak due to the absorption of C—H of benzene were also observed. Harmonic bands between 1900 and 2600 $cm^{-1}$ appeared.

The thermooxidative degradation of the polymer induced by heating in air was reflected by the changes observed in the spectra of the degraded samples. After heating in air, which occurred during the re-fusion process, bands were observed in the spectra of the quenched or air-cooled PET coatings around 3400 and 3200 $cm^{-1}$, which suggested the hydroxylation of the terephthalic ring yielding hydroxylated species (Fig. 9).

In the spectra of the quenched and air-cooled 80% PET/20% EMAA coatings on steel (Fig. 10), the air-cooled 90% PET/20% EMAA coating, and the 70% PET/20% EMAA coating on steel, a broad band was observed around 3270 $cm^{-1}$, which suggested the hydroxylation of the terephthalic ring.[33] The hypothesis of the hydroxylation of the degraded PET samples was reinforced by the appearance or increase in the intensity of the peaks at 1371 $cm^{-1}$, which were

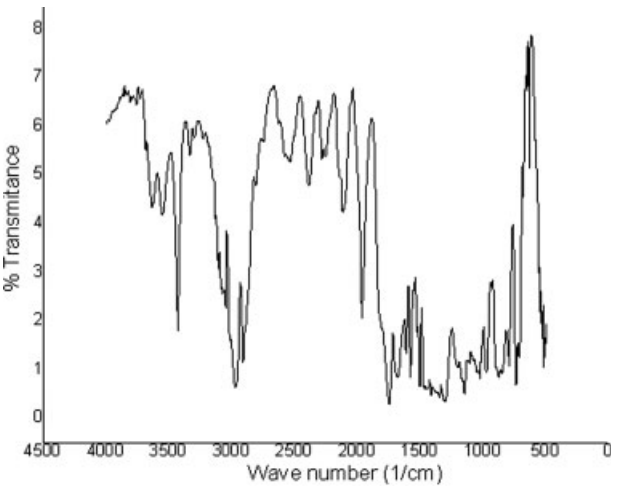


**Figure 8** FTIR spectrum of the PET powder.

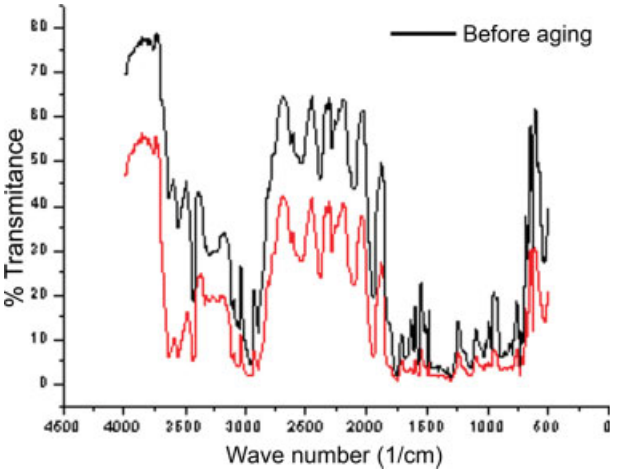


**Figure 9** FTIR spectra of quenched and re-fused PET coated before and after the aging process. [Color figure can be viewed in the online issue, which is available at www.interscience.wiley.com.]

assigned to the phenolic —OH, and 1174 $cm^{-1}$, which was attributed to aromatic OH deformation (Figs. 8 and 10). A similar observation was reported by Edge et al.[20,21] in their investigation of the extracts of PET samples degraded in air at 300°C. The band around 3300 $cm^{-1}$ was not present when the heating was carried out in nitrogen, which suggested that hydroxylation occurred when oxygen was present.[20,21]

After aging, the quenched and air-cooled PET coatings on steel did not show the peak at 3200 $cm^{-1}$, and the peak at 3400 $cm^{-1}$decreased in intensity but showed a broad band around 3300 $cm^{-1}$, as shown in Figure 8. Ciolacu et al.[33] reported that after heating in air, a broad band around 3270 $cm^{-1}$ was observed in the spectrum of degraded PET samples, which suggested the hydroxylation of the terephthalate ring yielding hydroxylated species. Earlier studies carried out by Edge et al.[20,21] suggested that color formation starts with the hydroxylation of the terephthalate ring producing hydroxylated species, which on further oxidation, leads to quinonoid-type structures. A color change on the coating surface was observed for PET and the blend coatings on steel (Figs. 1 and 3).

The quenched PET coatings on steel and the quenched 80% PET/20% EMAA blend coatings showed a loss of brightness and color alteration with the generation of a white color on the surface of the aged samples. The fine white layer produced on the surface of the quenched PET coatings after aging was probably due to a crystallization process. The temperature in the chamber was up to 70°C and was lightly higher than the glass-transition temperatures measured for PET and the PET/EMAA blends, which occurred in the range 62–69°C.[30] The time of exposure of 807 h could also have initiated the crystallization of PET. After the aging process, the coated steels were also analyzed with DSC.[30] An important result found was the increase in the glass-transition temperatures of the aged coatings, which may have indicated a crosslinking process, a hydrogen bond network, or crystallization operating during exposure in the weathering chamber. After exposure in the weathering chamber, the glass-transition temperature increased from 68 to 76°C for the quenched PET coating.[30] The crystallization fractions of the PET powder and the air-cooled thermally sprayed PET coatings were 41 and 21%, respectively.[34] The deposition process probably caused a recrystallization of the PET, and the crystallization fraction decreased.[34] The crystallization grade of the coating depended on the cooling rate and the molecular mass of the polymer.[34] In a previous work,[30] the crystallization fraction measured of the PET powder used in this study was 42% and decreased to the range 17–21% for the PET–EMAA blend coatings. The crystallization fractions of the quenched 80% PET/20% EMAA coatings before and after the aging process were 19 and 21%, respectively,[30] with a probable crystallization of the quenched PET in the weathering chamber. However, the crystallization fraction of the quenched PET coatings did not change and was 26% before and after exposure in the weathering chamber.[30]

The peak at 3650 $cm^{-1}$, which was not identified in the spectra of the air-cooled re-fused PET coating before aging, was identified in the PET sample after aging (Fig. 11). The spectra of the PET coating after aging (Fig. 11) showed peaks at 3550 $cm^{-1}$associated with absorbed moisture, 3440 $cm^{-1}$ related to the

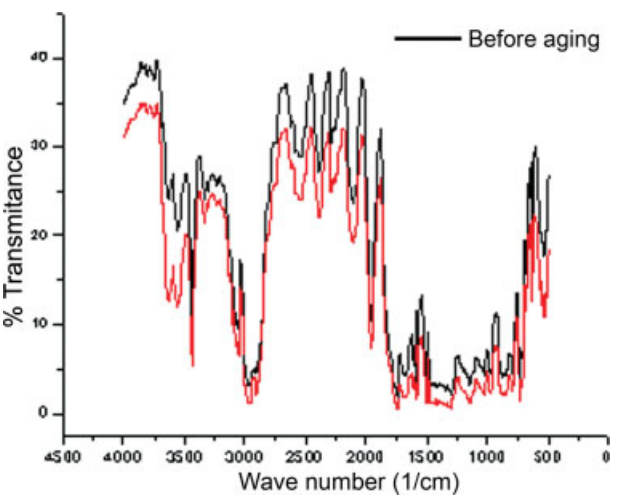


**Figure 10** FTIR spectra of air-cooled 80% PET/20% EMAA before and after the aging process. [Color figure can be viewed in the online issue, which is available at www.interscience.wiley.com.]

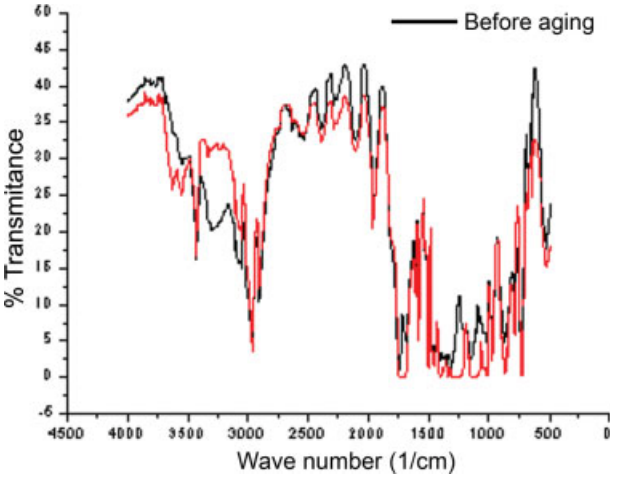


**Figure 11** FTIR spectra of air-cooled PET before and after the aging process. [Color figure can be viewed in the online issue, which is available at www.interscience.wiley.com.]

O—H stretching of ethylene glycol end groups, and 2980–2920 $cm^{-1}$ associated with aliphatic C—H stretching.

In the spectra of the air-cooled re-fused PET coating before aging (Fig. 11) and the spectra of the quenched re-fused PET coating after aging obtained with spectroscopy with the ZnSe crystal, peaks at 2980–2920, 1730, 1260, 1130, and 730 $cm^{-1}$ were observed according to the typical PET spectra. In the spectra of the quenched and air-cooled re-fused PET coatings after aging, there was observed an alteration in relation to the spectrum of the PET powder (Fig. 8) with the appearance of a peak at 1550 $cm^{-1}$. The peak around 1550 $cm^{-1}$ was clearly identified in the spectra of the quenched and air-cooled 80% PET/20% EMAA coatings before the aging process, in the spectra of the 90% PET blend coating before and after aging, and in the spectra of the 70% PET/30% EMAA coating mainly before aging. This peak may have been related to unsaturations in the polymeric chains, according to Edge et al.[20] These unsaturations may have been due to the degradation process. Holland and Jay[16,17] reported that the band at 1560 $cm^{-1}$ was related to the buildup of a conjugated aromatic structure in the polymer. The appearance of the new infrared band evolved at 1560 $cm^{-1}$ coincided with changes in the C—H (deformation) region at 950–750 $cm^{-1}$ of the infrared spectra. The changes observed in the C—H (deformation) region at 880 and 823 $cm^{-1}$ may have indicated that the structure of the aromatic ring changed from 1,4 to 1,3 positions. Edge et al.[20] also observed bands near 800 $cm^{-1}$ that signified alterations in the positions of the aromatic ring of PET. An intense band at 823 $cm^{-1}$ was observed in the spectra of the quenched and air-cooled 80% PET blend coatings before and after aging (Fig. 10), the air-cooled 90% PET blend coatings before and after aging, the quenched re-fused PET before the aging process (Fig. 9), and the 70% PET blend coatings.

The peaks between 1600 and 1650 $cm^{-1}$ was associated with aromatic ketones and α–β unsaturated carbonyl.[20] These peaks were identified in the spectra of the quenched (Fig. 9) and air-cooled re-fused PET coatings, the quenched 80% PET coating before aging, the air-cooled 90% PET blend coating before and after aging, the 70% PET blend coating, and the air-cooled 80% PET blend coating (Fig. 10).

For all samples, the chemical structure of the PET was maintained.

The spectra of the blend coatings (Fig. 10) showed peaks at 3550, 3650, 3440, 3300–3200, and 2980–2920 $cm^{-1}$ and the harmonic bands that are characteristic of PET.

Ultraviolet–visible spectroscopy was used for all of the samples. With ultraviolet–visible spectroscopy, the yellowness index can be estimated by the increase in the absorption at 400 nm. This increase is mainly due to quinone and diquinone formed during the photodegradation of PET.[21] The ultraviolet spectra of the blend coatings after the aging process showed a higher value of reflectance than the spectra of the coatings before aging (Fig. 12).

In all spectra, a peak at 360 nm was observed and attributed to the sensibility of the detector to the change from the tungsten lamp to the deuterium lamp. We also observed a peak at 740 nm due to the change of equipment detector.

In the spectra of EMAA and the PET–EMAA blends (Fig. 12), we observed a peak at 225 nm associated with the carboxyl conjugated with a double bond between carbon atoms, which produced a dis-

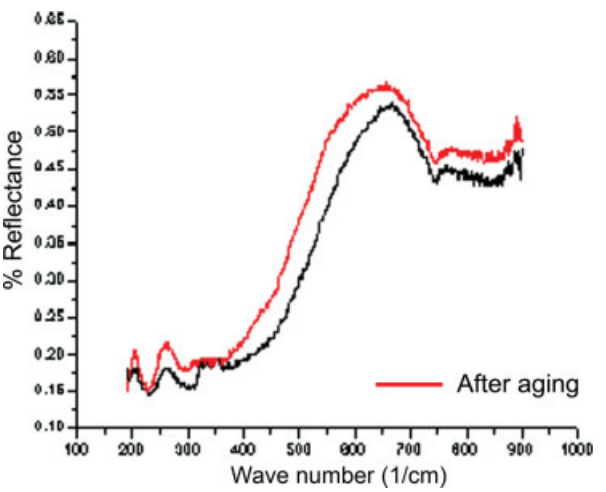


**Figure 12** Ultraviolet–visible spectra of air-cooled 80% PET/20% EMAA before and after the aging process. [Color figure can be viewed in the online issue, which is available at www.interscience.wiley.com.]

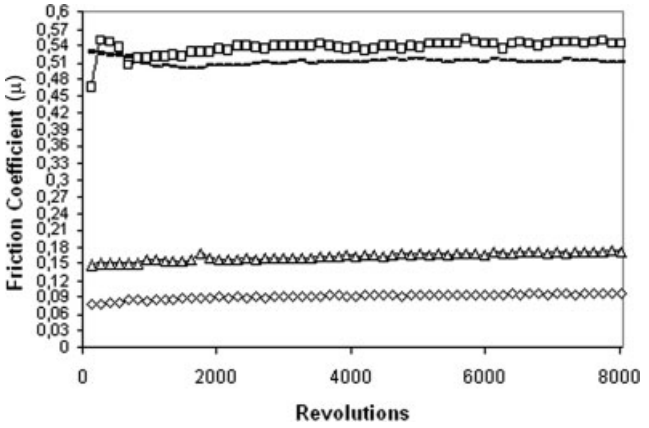


**Figure 13** Friction coefficient of the polymeric coatings.

location in the maximum wave number. In the spectra of the re-fused PET coating, there was a peak at 240 nm and a peak at 300 nm that could have been associated with the aromatic ring linked to the carboxyl acid ended or ester with the presence of chromophorous groups linked to the benzenic ring produced bands at higher wave numbers. We also observed a peak at 490–505 nm in the spectroscopy spectra of the samples before aging.[31] The amorphous samples of the quenched PET coatings before and after aging showed a peak at 195 nm associated with the aromatic compounds.

In the spectra of the 90% PET/EMAA, 80% PET/EMAA, and 70% PET–EMAA blend coatings and the EMAA coatings, peaks of both polymers were identified. The peaks at 225 nm of the EMAA and the peak at 240 nm of the PET were overcome. The peak at 300 nm associated with the aromatic ring linked to the carboxyl acid ended and to the ester, which was characteristic of the PET structure, was clearly identified in the blend spectra.

### Tribological tests

Figure 13 shows the friction coefficient of the coatings as a function of the revolution number, and the hardness tests results are shown in Figure 2.

The EMAA coating samples, which were produced with the fusion technique and the thermal spraying process, showed the greatest coefficient value with respect to the coatings studied. EMAA was less stiff and more elastic than PET. This elasticity increased the sliding resistance of the pin.

The quenched PET coating samples showed the smallest friction coefficient of all of the samples. Branco et al.[35] reported that during pin-on-disc testing, the friction coefficient of thermally sprayed PET coatings varies between 0.1 and 0.3. Branco et al.[35] reported that scratches are the predominant tribographic features inside the wear track, and they are continuous and concentric. Debris is spread in the wear tracks, especially on their outside edges. Branco et al.[35] showed evidence that the pin-on-disk wear develops an abrasion process, through a ploughing mechanism, although a fatigue mechanism could not be disregarded. The low friction coefficient previously observed between PET and steel was confirmed. Branco et al.[35] showed that friction force is very sensitive to the presence of the polymer debris at the pin–PET interface and increases as the debris content increases and decrease once it is released; this promotes friction fluctuation during sliding. In the as-sprayed condition, the PET coatings showed higher friction, which was likely because of a higher coarse debris production rate during the pin-on-disk testing. Quenching the as-sprayed coating to increase the amorphous PET content improved the sliding behavior by increasing the wear resistance. The friction coefficients of the polymeric coatings obtained in this study agreed with the literature data.[35]

The results indicated that EMAA addition did not significantly increase the PET elasticity, and the blend-coating samples presented similar behavior to the PET coating samples.

In general, there were two kinds of wear.[36] The first was the adhesion of EMAA, and the other was the cohesion of the PET and blends. Adhesion occurred when the coating was worn, separated, and stuck to the pin. Cohesion occurred when the coating did not separate but formed a high border.

The EMAA coating samples showed a high value of the friction coefficient, and their wear behavior differed from that of PET and the PET/EMAA blend coating samples.

## CONCLUSIONS

Quenched PET blends with 80% PET and quenched PET coatings showed some characteristics, such as corrosion resistance in a salt-spray chamber, a small friction coefficient, and adhesion, which are necessary to the application of these polymeric films as protective coatings against corrosion and wear.

After the aging process of the thermally sprayed EMAA coatings, the duplications of the peaks at 1260 and 940 and 960 $cm^{-1}$ were observed. The peak at 1260 $cm^{-1}$ was associated with the C—O bond, and the peaks at 960 and 940 $cm^{-1}$ were associated with the O—H and appeared because of the hydration of the carboxyl.

After heating in air, which occurred during the refusion process, bands were observed in the spectra of the quenched and air-cooled PET coatings around 3400 and 3200 $cm^{-1}$, which suggested hydroxylation

of the terephthalic ring yielding hydroxylated species.

In the spectra of the quenched and air-cooled 80% PET/20% EMAA coatings on steel, the air-cooled 90% PET/20% EMAA coating, and the 70% PET/20% EMAA coating on steel, a broad band was observed around 3270 $cm^{-1}$, which suggested hydroxylation of the terephthalic ring.

The hypothesis of the hydroxylation of the degraded PET samples was reinforced by the appearance or the increase of the intensity of peaks at 1371 $cm^{-1}$ assigned to the phenolic —OH, and at 1174 $cm^{-1}$ attributed to aromatic OH deformation.

The quenched PET coatings on steel and the quenched 80% PET/20% EMAA blend coatings showed a loss of brightness and color alteration with the generation of a white color on the surface of the aged samples.

In the spectra of the quenched and air-cooled refused PET coating after aging, there was observed an alteration in relation to the spectrum of PET powder with the appearance of a peak at 1550 $cm^{-1}$. The peak around 1550 $cm^{-1}$ was clearly identified in the spectra of the quenched and air-cooled 80% PET/20% EMAA coatings before the aging process, the 90% PET blend coating before and after aging, and the 70%PET/30% EMAA coating mainly before aging. This peak may have been related to unsaturations in the polymeric chains. These unsaturations may have been due to the degradation process.

Ultraviolet spectra of the blend coatings after the aging process showed a higher value of reflectance than the spectra of the coatings before aging.

The authors are grateful to Energetic Co. of Minas Gerais for supplying the aging test equipment.

## References


1. Varacalle, D. J.; Couch, K. W.; Budinger, V. S. In Proceedings of the 9th National Thermal Spray Conference, Cincinatti, OH, 1996; pp 251–255.
2. Kawase, R.; Nakano, A. In Proceedings of the 9th National Thermal Spray Conference, Cincinatti, OH, 1996; pp 257–262.
3. Brogan, J. A. Ph.D. Thesis, State University of New York at Stony Brook, 1996.
4. Kenny, E. D.; Esmanhoto, E. J. In Proceedings of the 8th Brazilian Meeting of Surface Treatment - EBRAT'S 94, Brazilian Association of Surface Treatment, São Paulo, Brazil, 1994.
5. Saha, B.; Ghoshal, A. K. Chem Eng J 2005, 111, 39.
6. Girija, B. G.; Sailaja, R. R. N.; Madras, G. Polym Degrad Stab 2005, 90, 147.
7. Loustannau, P. J.; Horton, D. Mater Perform 1994, 33, 32.
8. Kenney, J. F.; Haddock, T. H.; Sun, R. L.; Parreira, H. C. J Appl Polym Sci 1992, 45, 355.
9. Billmeyer, F. W. J. Textbook of Polymer Science; Wiley: New York, 1992.
10. Mark, H. F.; Bikales, N. M.; Overberger, C. G.; Menges, G. Encyclopedia of Polymer Science and Engineering; Wiley: New York, 1990.
11. Shalaby, S. W. J Polym Sci Macromol Rev 1979, 14, 419.
12. Carlsson, D. J.; Wiles, D. M. J Macromol Sci Rev Macromol Chem 1976, 65, 65.
13. Rabek, J. F. Polymer Photodegradation: Mechanisms and Experimental Methods; Chapman & Hall: London, 1995.
14. Fechini, G. J. M.; Rabello, M. S.; Souto-Maior, R. M. Polym Degrad Stab 2002, 75, 153.
15. Samperi, F.; Puglisi, C.; Alicata, R.; Montaudo, G. Polym Degrad Stab 2004, 83, 3.
16. Holland, B. J.; Hay, J. N. Polymer 2002, 43, 1835.
17. Holland, B. J.; Hay, J. N. Polymer 2002, 43, 1797.
18. Botelho, G.; Queiros, A.; Liberal, S.; Gijsman, P. Polym Degrad Stab 2002, 74, 39.
19. Dzieciol, M.; Trzeszczynski, J. J Appl Polym Sci 2000, 77, 1894.
20. Edge, M.; Wiles, R.; Allen, N. S.; McDonald, W. A.; Mortlock, S. V. Polym Degrad Stab 1996, 53, 141.
21. Edge, M.; Wiles, R.; Allen, N. S.; McDonald, W. A.; Mortlock, S. V. Polymer 1995, 36, 227.
22. Blais, D.; Day, M.; Wiles, D. M. J Appl Polym Sci 1973, 17, 1895.
23. Day, M.; Wiles, D. M. J Appl Polym Sci 1972, 16, 175.
24. Allen, N. S.; Edge, M.; Mohammadian, M. Polym Degrad Stab 1994, 43, 229.
25. Foti, S.; Gruffreda, M.; Maravigna, P.; Montaudo, G. J Polym Sci Polym Chem 1984, 22, 1217.
26. Kalfoglou, N. K.; Skafidas, D. S. Eur Polym J 1994, 30, 23.
27. Subramanian, P. M. In Proceedings of the Symposium on New Developments in Plastic Recycling, University of North Carolina, Charlotte, NC, 1989; p 30.
28. Roberge, P. Handbook of Corrosion Engineering; McGraw-Hill Professional: New York, 1999.
29. Silverstein, R. M.; Webster, X. F. Identificação Espectrométrica de Compostos Orgânicos; LTC Editora: Rio de Janeiro, 2000.
30. Cury, F. M. M.S. Thesis, Federal University of Minas Gerais, 2005.
31. Oreski, G.; Wallner, G. M. Sol Energy 2005, 79, 612.
32. Duarte, L. T.; Paula e Silva, E. M.; Branco, J. R. T.; Lins, V. F. C. Surf Coat Technol 2004, 182, 261.
33. Ciolacu, C. F. L.; Choudhury, N. R.; Dutta, N. K. Polym Degrad Stab 2006, 91, 875.
34. Duarte, L. T.; Mariano, C.; Branco, J. R. T.; Collares, M. P.; Gallery, R.; Lins, V. F. C. Polím Ciênc Tecnol 2003, 13, 95.
35. Branco, J. R. T.; Campos, S. R. V.; Duarte, L. T.; Lins, V. F. C. J Appl Polym Sci 2004, 92, 3159.
36. Hutchings, I. M. Tribology: Friction and Wear of Engineering Materials; CRC: London, 1992.